PERIODIC ORBITS, SYMBOLIC DYNAMICS AND TOPOLOGICAL ENTROPY FOR THE RESTRICTED 3-BODY PROBLEM

GIANNI ARIOLI

Abstract. This paper concerns the restricted 3-body problem. By applying topological methods we give a computer assisted proof of the existence of some classes of periodic orbits, the existence of symbolic dynamics on five symbols and we give a rigorous lower estimate for the topological entropy.

1. Introduction

The periodic problem for both restricted and full N-body systems has such a long story that it is impossible to give an extensive bibliography here; we refer the reader to the classical texts [MH, M, MS, S].

This paper concerns the planar restricted 3-body problem. If we assume that the primaries orbit around each other with period 2π and we use a rotating reference frame, i.e. if we use synodical coordinates, then the motion of the third body is described by the following system of second order differential equations:

$$\begin{aligned} \ddot{x} + 2\dot{y} &= \Omega_x \\ \ddot{y} - 2\dot{x} &= \Omega_y, \end{aligned} \tag{1.1}$$

where

$$\Omega(x,y) = \frac{x^2}{2} + \frac{y^2}{2} + \frac{m_1}{\sqrt{(x-R_1)^2+y^2}} + \frac{m_2}{\sqrt{(x+R_2)^2+y^2}} + C,$$

m_1 and m_2 are the masses of the primaries, C is a constant we choose for convenience and R_1, R_2 depend on m_1 and m_2.

The methods we employ are topological with computer assistance. This kind of computer assisted proof was introduced in [MM1, MM2, MM3], while the topological methods employed here have been introduced in [Z1, Z2], see also the applications in [AZ, GZ, Z3].

The purpose of the paper is fourfold: we discuss how the computer assisted techniques can provide results for this problem; we give a rigorous proof of the existence of a class of periodic orbits at different energy levels; we prove the existence of symbolic dynamics on five symbols and we provide a lower estimate for the topological entropy.

2. Description of the system

We first derive briefly equation (1.1). It is well known that the two body problem admits a solution where both bodies move in a circular anticlockwise motion around their center of mass (and of course it also admits the symmetric clockwise solution). We call the two bodies P_1 and

This research was supported by MURST project "Metodi variazionali ed Equazioni Differenziali Non Lineari".

P_2 (the primaries). If P_1 and P_2 have mass m_1 and m_2, then the circular solution with minimal period 2π minimizes the Lagrangian functional

$$f(x_1, x_2) := \int_0^{2\pi} \frac{m_1}{2}|\dot{x}_1|^2 + \frac{m_2}{2}|\dot{x}_2|^2 + \frac{m_1 m_2}{|x_1 - x_2|}.$$

Take

$$x_1 = R_1(\cos t, -\sin t) \text{ and } x_2 = R_2(-\cos t, \sin t);$$

in order to compute R_1 and R_2 we have to minimize

$$\tilde{f}(R_1, R_2) = \frac{m_1}{2}R_1^2 + \frac{m_2}{2}R_2^2 + \frac{m_1 m_2}{R_1 + R_2}. \tag{2.1}$$

Setting 0 as the center of mass we have $R_2 = \frac{m_1}{m_2}R_1$, and by minimizing $\tilde{f}(R_1, R_2)$ we get $R_1 = \frac{m_2}{(m_1+m_2)^{2/3}}$ and $R_2 = \frac{m_1}{(m_1+m_2)^{2/3}}$. If the masses are equal, then $R_1 = R_2 = 2^{-2/3}$; if $m_1 = 1$ and $m_2 = 2$, then $R_1 = 2\left(3^{-2/3}\right)$ and $R_2 = 3^{-2/3}$. We only consider these two cases. The reason for this choice is that the case of equal masses has been already considered and periodic orbits for this case are known to exist; nonetheless, rigorous estimates on the location of the orbits and results on symbolic dynamics and topological entropy are new to the author knowledge. Furthermore the equal masses case is, in some sense, the opposite of a "perturbative" case with one primary much less massive than the other one. The case $m_1 = 1$ and $m_2 = 2$ is considered only on a numerical level to show whether the symmetry between the masses influences the qualitative behavior of the system.

The Lagrangian for the restricted 3-body problem is $\tilde{L}(w) = \frac{1}{2}|\dot{w}|^2 - V(w)$ where

$$V(w) = -\frac{m_1}{|w - x_1|} - \frac{m_2}{|w - x_2|}.$$

We find it convenient to use synodical coordinates, i.e. a reference frame where the primaries sit still. Set $w = Rv$, where $R = \begin{pmatrix} \cos t & \sin t \\ -\sin t & \cos t \end{pmatrix}$ and let $J = \begin{pmatrix} 0 & -1 \\ 1 & 0 \end{pmatrix}$ be the standard symplectic matrix; then $\dot{w} = \dot{R}v + R\dot{v} = R(\dot{v} - Jv)$, therefore the Lagrangian is given by

$$L(v) = \frac{1}{2}|\dot{v}|^2 - (\dot{v}, Jv) + \Omega(v),$$

where

$$\Omega(v) = \frac{|v|^2}{2} + \frac{m_1}{|v - (R_1, 0)|} + \frac{m_2}{|v - (-R_2, 0)|} - C \tag{2.2}$$

It is well known that $H(x, \dot{x}, y, \dot{y}) = \dot{x}^2 + \dot{y}^2 - 2\Omega(x, y)$ is an integral of the motion (the Jacobi integral), therefore the motion takes place on the manifold $H(x, \dot{x}, y, \dot{y}) = h$. With some abuse of language, we call the Jacobi integral $H(v) = |\dot{v}|^2 - 2\Omega(v)$ the *energy*. The Euler-Lagrange equations are:

$$\ddot{v} - 2J\dot{v} - \nabla\Omega(v) = 0. \tag{2.3}$$

This system admits five equilibrium points. Three such points are aligned with the primaries and are called L_1, L_2 and L_3 (the collinear equilibrium solutions), One of the collinear points lies between the primaries; let that point be L_1. All the collinear points are saddles for Ω. The remaining two equilibrium points are called L_4 and L_5; they are the absolute minima of Ω and they both sit at the vertices of an equilateral triangle with the primaries at the other vertices (the equilateral equilibrium solutions). We choose the constant C in order to have

$\Omega(L_1) = 0$. By a direct computation it is easy to see that there exists $h_0 > 0$ such that the region $\{v : 2\Omega(v) + h \geq 0\}$ where the motion can take place is split in exactly two connected regions, one bounded and the other unbounded, if and only if $0 \leq h < h_0$. We call the bounded region *admissible* and we look for trajectories in the admissible region. In both the cases we consider it turns out that h_0 is close to 0.85. We only consider values of h in the range $[0, h_0)$. Note that, if $h = 0$, the bounded region consists in two sets connected at the origin and no trajectory can intersect both sets; if $0 < h < h_0$ the admissible region is homeomorphic to a ball (if we include the singularities in the region); if $h < 0$ there are three connected regions and finally if $h \geq h_0$ the region $2\Omega(v) + h \geq 0$ is connected (but not simply connected). The following pictures represent the curves $\{2\Omega(v) + h = 0\}$ for different values of h:

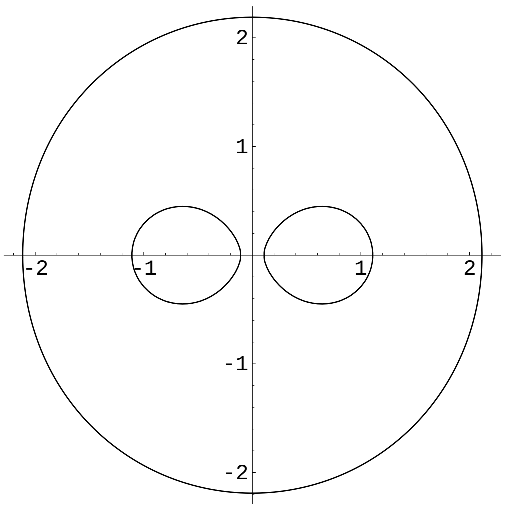

$h = -.2$

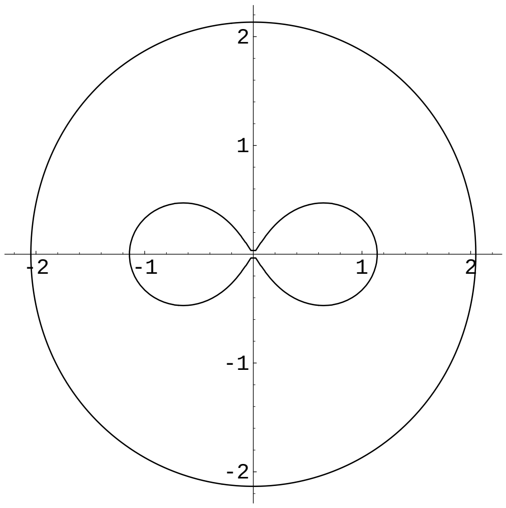

$h = 0$

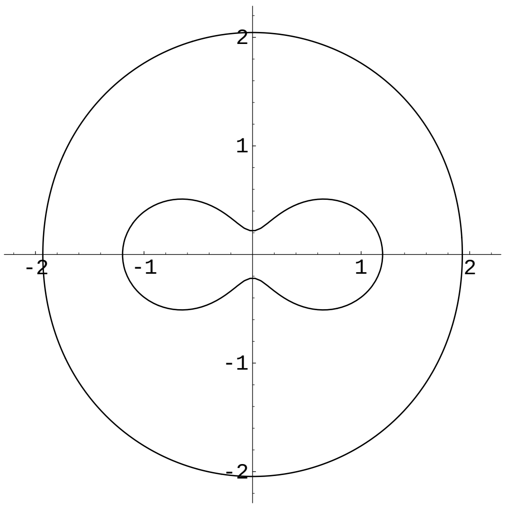

$h = .3$

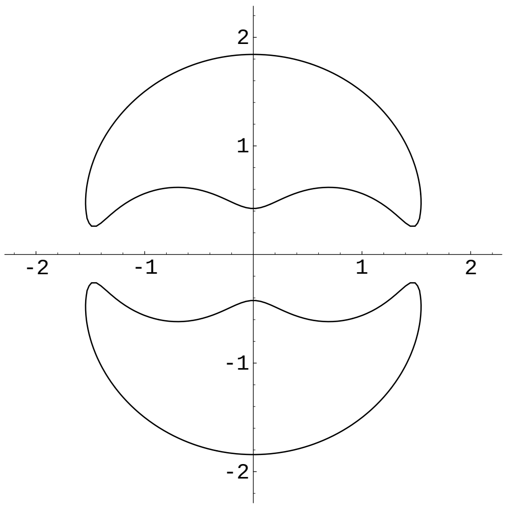

$h = .9$

3. The Poincaré maps

In order to study the system at some fixed energy h we consider the Poincaré return map $P : D(P) \subset \mathbb{R}^2 \to \mathbb{R}^2$ defined in the following way. Given (x, p_x) such that $x \neq \{R_1, -R_2\}$ and $2\Omega(x,0) + h - p_x^2 > 0$ there exists a unique positive value of $p_y = p_y(x, p_x) = \sqrt{2\Omega(x,0) + h - p_x^2}$ such that $H(x, p_x, 0, p_y) = h$. Let $\varphi(x, p_x; \cdot) : \mathbb{R} \to \mathbb{R}^4$ be the solution of the equation (1.1) with initial conditions $x(0) = x$, $\dot{x}(0) = p_x$, $y(0) = 0$, $\dot{y}(0) = p_y$ and call φ_i, $i = 1, \ldots, 4$ its components. By definition $\varphi_3(x, p_x; 0) = 0$ and $\varphi_4(x, p_x; 0) > 0$, therefore $\varphi_3(x, p_x; t) > 0$ for all positive and small t. If there exists a time T_1 such that $\varphi_3(x, p_x; T_1) = 0$ and $\varphi_3(x, p_x; t) > 0$ for all $t \in (0, T_1)$, and a time $T_2 > T_1$ such that $\varphi_3(x, p_x; T_2) = 0$ and $\varphi_3(x, p_x; t) < 0$ for all $t \in (T_1, T_2)$, then we define

$$P(x, p_x) = (\varphi_1(x, p_x; T_2), \varphi_2(x, p_x; T_2)).$$

In other words, P is the return map on the section $y = 0$, $p_y > 0$.

In fact, for different reasons which we point out later, we find it useful to consider the half Poincaré maps $H_1 : D(H_1) \subset \mathbb{R}^2 \to \mathbb{R}^2$ and $H_2 : D(H_2) \subset \mathbb{R}^2 \to \mathbb{R}^2$. H_1 is defined by

$$H_1(x, p_x) = (\varphi_1(x, p_x; T_1), \varphi_2(x, p_x; T_1)),$$

where the maps φ and the time T_1 are as before, while H_2 is defined by

$$H_2(x, p_x) = (\tilde{\varphi}_1(x, p_x; T_1), \tilde{\varphi}_2(x, p_x; T_1)),$$

where $\tilde{\varphi}(x, p_x; \cdot) : \mathbb{R} \to \mathbb{R}^4$ is the solution of the equation (1.1) with initial conditions $x(0) = x$, $\dot{x}(0) = p_x$, $y(0) = 0$, $\dot{y}(0) = -\sqrt{2\Omega(x,0) + h - p_x^2}$ and $T_1 > 0$ is such that $\varphi_3(x, p_x; T_1) = 0$ and $\varphi_3(x, p_x; t) < 0$ for all $t \in (0, T_1)$. Of course, $D(P) \subset D(H_1)$, $H_1(D(P)) \subset D(H_2)$ and $P = H_2 \circ H_1$. In the following we refer to the maps H_1 and H_2 as the first and second half Poincaré maps respectively. In other words the map H_1 (resp. H_2) is the transition map from the section $y = 0$, $p_y > 0$ to the section $y = 0$, $p_y < 0$ (resp. from the section $y = 0$, $p_y < 0$ to the section $y = 0$, $p_y > 0$).

By inspection it is easy to see that, if $(x(t), y(t))$ is a solution of 1.1, then $(\tilde{x}(t), \tilde{y}(t)) := (x(-t), -y(-t))$ is also a solution. This implies that $H_1(x_1, p_1) = (x_2, p_2)$ is equivalent to $H_2(x_2, -p_2) = (x_1, -p_1)$ and $P(x_1, p_1) = (x_2, p_2)$ is equivalent to $P(x_1, -p_2) = (x_2, -p_1)$.

4. Periodic orbits

A standard method for studying periodic orbits consists in looking for fixed points of the Poincaré map P. By the symmetry of the system considered at the end of the previous section we infer that $H_1(x_1, 0) = (x_2, 0)$ yields $H_2(x_2, 0) = (x_1, 0)$, which in turn implies that $(x_1, 0)$ is a fixed point for the Poincaré map. On the other hand, if the system admits a periodic orbit which crosses orthogonally the x-axis at some point x_1, then, by definition of Poincaré map, $P(x_1, 0) = (x_1, 0)$, and this is possible only if $H_1(x_1, 0) = (x_2, 0)$ for some x_2. It turns out that it is also fruitful to consider whether there exist points x_1 and x_2 such that $P(x_1, 0) = (x_2, 0)$, with $x_1 \neq x_2$. By the same reason as before, these points correspond to periodic points of period 2 for the Poincaré map, hence to periodic trajectories for the system crossing the $y = 0$ hyperplane at two different points in each direction, see the picture in the following section.

Let $f(x)$ be the second component of $H_1(x, 0)$ and $g(x)$ be the second component of $P(x, 0)$. In order to find fixed or periodic points for the Poincaré map we can look for zeros of the function f or g. We remark that, even by considering the map g only, one can still find all the periodic orbits which cross orthogonally the x-axis. On the other hand it may happen that $P(x_1, 0) = (x_2, 0)$ with x_1 very close to x_2, in the sense that $|x_1 - x_2|$ is smaller than the numerical error. In this case it is impossible to find out whether x_1 is a fixed point or a periodic point of period 2, without considering the derivative of the Poincaré map. For this reason it is convenient to study both the map f and the map g. The following picture displays $f(x)$ with $x \in (-.62, .62)$ and $h = .1$ in the case $m_1 = m_2 = 1$.

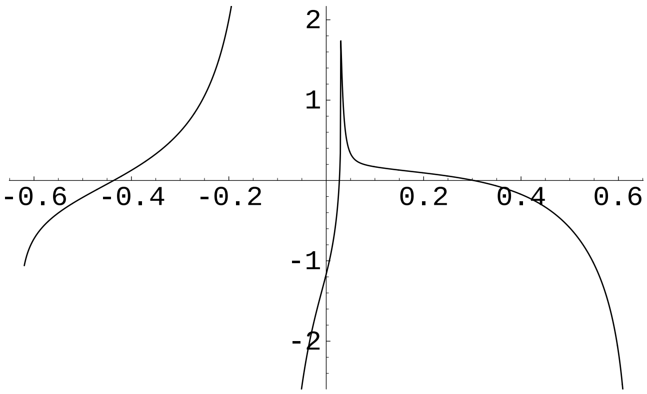

$h = .1$

The picture strongly suggests that the Poincaré map has three fixed points in the set $\{(x, 0) : x \in (-.62, .62)$, which is exactly the result we show rigorously in the next section, where we also give a narrow bound on the position of such points. We now show how new periodic points are born, even if in this paper we just give an euristic picture and do not investigate this phenomenon any further. The next two pictures display the function f in the cases $h = .3$ and $h = .5$, still in the case $m_1 = m_2 = 1$. There is strong evidence that the image of the portion of the x-axis we consider tilts as h increases, raising new intersections; on the other hand, when h further increases, the graph leaves the x-axis, and two periodic orbits collapse into one and disappear.

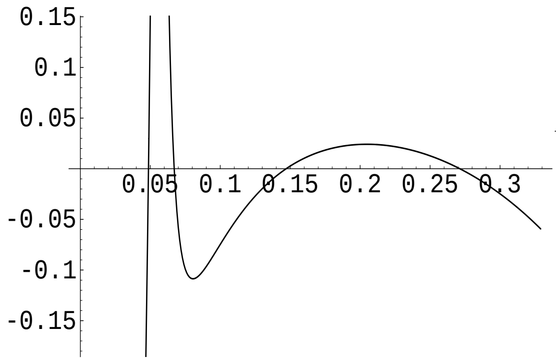

$h = .3$

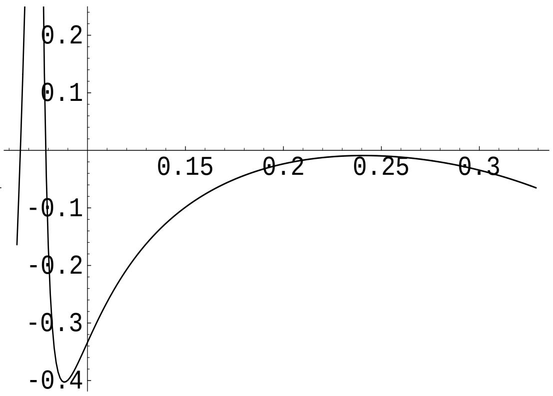

$h = .5$

The procedure outlined above leads to orbits which are approximately periodic, but is not a proof of the existence of periodic orbits. On the other hand the numerical computation of the Poincaré map with rigorous bounds on the error of computation can yield a rigorous result of existence. Our strategy is as follows: first we compute an approximate image of the x axis through the maps f and g as in the previous pictures; in this way we can spot the places where the intersections should be located. Assume that we conjecture the existence of a fixed point for P nearby some point $(\bar{x}, 0)$. We choose x_1 and x_2 such that $x_1 < \bar{x} < x_2$ and both x_1 and x_2 are very close to $\bar{x}$. Then we compute the rigorous half Poincaré map H_1 at $(x_1, 0)$ and $(x_2, 0)$. If we can prove that the second component of $H_1(x_1, 0)$ has opposite sign of the second component $H_1(x_2, 0)$ and that the segment joining the two points belongs entirely to the domain of H_1, then by the continuity of the half Poincaré map we have proved that there exists at least a point $x_1 < \tilde{x} < x_2$ such that $H_1(\tilde{x}, 0)$ lies on the x axis, therefore a periodic orbit passes through $(\tilde{x}, 0)$. On the other hand, if we prove that some portion of the x-axis is mapped away from the x-axis itself, then we have a proof that there are no periodic solutions which cross the x-axis orthogonally in that section. Then we move to the map P: we repeat the same procedure, but we only look for intersections that were not spotted for the map H_1. If we find two points x_1, x_2 such that the second component of $P(x_1, 0)$ lies on the opposite side of the x-axis with respect to the second component of $P(x_2, 0)$ and $H_1([x_1, x_2], 0)$ does not intersect the x-axis, then we have a proof that there exists at least a point $x_1 < \tilde{x} < x_2$ such that $\tilde{x}$ is the intersection of a period 2 orbit with the x-axis.

4.1. **Copenhagen orbits.** We first consider the case which is usually referred to as "the Copenhagen orbits", from the results of the Observatory of Copenhagen (see [S] and references therein), i.e. the case where $m_1 = m_2 = 1$. We recall that, by our choice of the constant C in (2.2), $h = 0$ is the energy of the stationary solution at the Lagrangian point L_1 (the origin). Since the problem has the additional symmetry consisting in switching the primaries, we only consider orbits that cross the portion of the x-axis between the primaries with positive speed in the y direction. The lowest value of h we consider is 0, when the admissible region is split in two parts touching at the origin and no trajectory can enter both regions. The highest value of h we consider is 0.8, since at slightly larger value the bounded admissible region touches the unbounded part and some trajectory starting close to the primaries may be unbounded.

h	S_1	S_2	L	D_1	D_2	U_1	U_2
0	0.3158	−0.4399					
.1	0.3028	−0.4365	0.02697				
.2	0.2883	−0.4330	0.03894				
.22	0.2851	−0.4323	0.04102				
.24	0.2818	−0.4316	0.04303			0.06963	0.1043
.26	0.2784	−0.4309	0.04497	0.04423	0.04456	0.06737	0.1205
.28	0.2749	−0.4301	0.04687	0.04600	0.04651	0.06689	0.1343
.3	0.2712	−0.4294	0.04873	0.04775	0.0484	0.06712	0.1470
.4	0.2443	−0.4257	0.05751	0.05615	0.05730	0.07199	0.2085
.5		−0.4218	0.06575	0.06412	**0.06546**	**0.07871**	
.6		−0.4178	0.07369	0.07185	**0.07344**	**0.08593**	
.8		−0.4093	0.08922	0.08716			

Table 1

The result we obtain are summarized in Table 1. In the left hand side column the energy level is displayed, while the remaining columns represent the intersection of the orbits with the x-axis. Orbits belonging to the same column appear to belong to the same class, in the sense that they have the same properties of stability, the same index with respect to the primaries and the Lagrangian point L_1. We wish to point out that part of these results are rigorous, in the sense that we have a computer assisted proof, while some other part is purely numerical

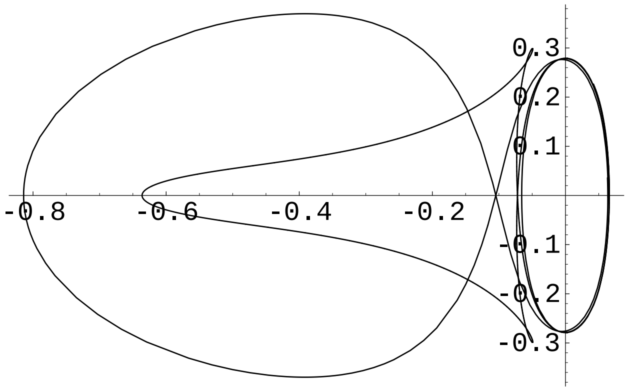

FIGURE 1. Orbits D_1, D_2 and L at energy level $h = .5$

or empirical. More precisely, the existence of the orbits is rigorous and the location is rigorous $\pm 5 \cdot 10^{-4}$, while the fact that they belong to the same branch is purely euristic, although very natural. By asserting that the location is rigorous $\pm 5 \cdot 10^{-4}$ we mean that we have a computer assisted proof that the second components of $H_1(x + 5 \cdot 10^{-4}, 0)$ and $H_1(x - 5 \cdot 10^{-4}, 0)$ have different sign and the interval set $[x - 5 \cdot 10^{-4}, x + 5 \cdot 10^{-4}] \times \{0\}$ is in the domain of H_1. The four orbits location denoted in bold characters are not verified rigorously, since the corresponding orbit is very close to one of the primaries and the rigorous numerical computation failed. The orbits in the class S_1 are retrograde around P_1; the orbits in the class S_2 are direct around P_1. The orbits in the class L are well known, they are retrograde and their trajectory is very close to an ellipse with center at the Lagrangian point L_1. They branch out from L_1, in the sense that as $h \to 0$ they collapse to L_1. These are the only orbit which have index 0 with respect to both primaries, and they have index 1 with respect to L_1. The orbits in the class D_i correspond to points of period 2 of the Poincaré map. In the following pictures the orbits D_1, D_2 and L at energy level $h = .5$ are displayed.

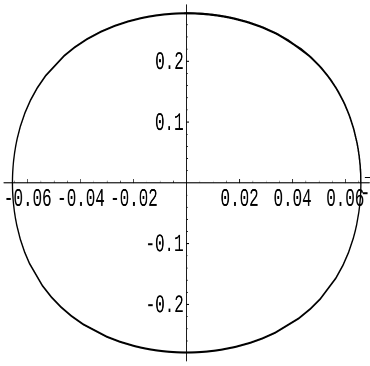

Orbit L

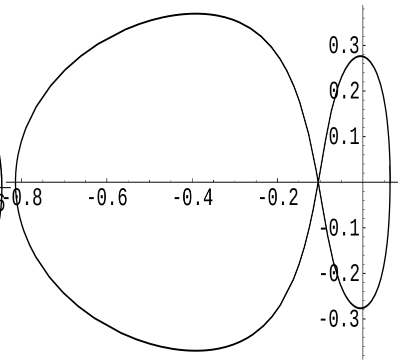

Orbit D_1

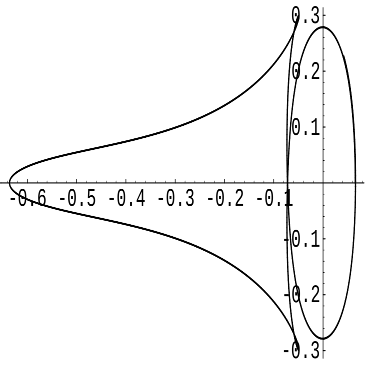

Orbit D_2

The same orbits are plotted together in Figure 1: note that part of the trajectories of both D_1 and D_2 are very close to the trajectory of L, giving a visual image of the strong instability of the system.

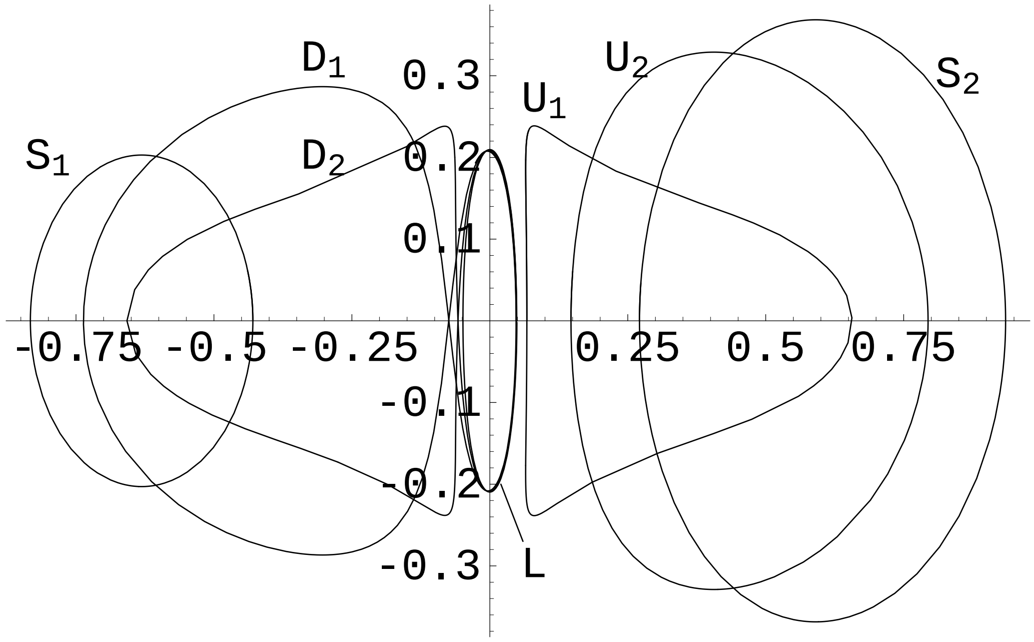

FIGURE 2. All orbits at $h = .3$

The following remarks are numerical or euristic, although we will give a computer assisted proof of bifurcations in a forthcoming paper. All orbits are unstable, except for orbits S_1 and S_2 which are linearly stable. The orbits D_1 and D_2 branch out from L at energy $h = .246$. The orbits in the classes U_1 and U_2 are unstable and direct; they appear as a single orbit at energy $h = .2242$ and then bifurcate. At energies higher than .6 both the orbit U_1 and D_2 degenerate into collision orbits. The orbits S_1 and U_2 collapse into each other at energy $h = .4144$ and then disappear. In Figure 2 we plot all periodic orbits at energy level $h = .3$.

4.2. **The case $m_1 = 1$ and $m_2 = 2$.** In order to check whether the symmetry is relevant to the results we obtained, we considered the case with $m_1 = 1$ and $m_2 = 2$. We obtain the following results, which are purely numerical (note that in this case $L_1 = (0.3424, 0))$:

	S_1	S_2	L	D_1	D_2	U_1	U_2
0	0.6590	-0.2317					
.1	0.6449	-0.2289	0.3708				
.15	0.6362	-0.2274	0.3777				
.2	0.6250	-0.2260	0.3838			0.4042	0.5093
.3		-0.2230	0.3943			0.4083	
.4		-0.2199	0.4038			0.4158	
.6		-0.2136	0.4211			0.4317	
.8	0.6008	-0.2069	0.4373	0.4360	0.4368		0.7467

As in the Copenhagen case, the orbits in the class L are the well-known orbits around the Lagrangian point L_1. At energies larger than 0.6 the orbit U_1 degenerates into a collision orbit. We note that the picture is very similar, but still it differs in some important qualitative points. The linearly stable orbits, i.e. the classes S_1 and S_2, are still there, and they look similar. The same holds for the unstable orbits, i.e. the classes U_1 and U_2: both these orbits appear as a single orbit at $h = .15254$ and bifurcate. As in the Copenhagen case the orbit S_1 and U_2 collapse into each other at $h = .26$, but they reappear at $h = .6646$. Of course the statement "the orbits reappear" is purely descriptive; on the other hand the behavior and the shape of the orbits is the same as for $h \leq .26$. As far as the other orbits are concerned, the qualitative picture is the same as before. These results are not rigorous: in a forthcoming paper we will provide a rigorous and more detailed picture of the dependence of the orbits to the masses of the primaries.

5. Chaotic dynamics

We apply the method developed in [Z1, Z2, Z3], see also [AZ] where the Hénon-Heiles Hamiltonian was concerned. We only consider the case with equal masses at energy $h = .3$. We prove the existence of symbolic dynamics on five symbols. More precisely, consider the unstable periodic orbits U_1, U_2, L, D_1 obtained in the previous section and the orbit symmetric to U_1 with respect to the y axis and associate a symbol to each orbit: we prove that, given any admissible (see Definition 5.7) biinfinite sequence of the five symbols introduced above, there exists a solution of the problem whose trajectory is close to the corresponding sequence of periodic orbits. Furthermore we give a lower estimate for the topological entropy.

The computation of rigorous estimates in the (restricted) 3-body problem presents more difficulties than the cases previously considered. The first is due to the fact that the Poincaré map is not defined in a connected region, indeed we have to exclude at least the lines $x = R_1$ and $x = -R_2$. This could be avoided by using some kind of regularization, but we prefer to keep the original coordinates, both because they are far more intuitive and because the Levi-Civita transform (or its variations) is not one to one. Furthermore, even after some kind of regularization, it is far from trivial to determine what is the domain of the Poincaré map. But the main problem is due to the fact that, even using a sofisticated algorithm to compute the rigorous bounds, such bounds turn out to be very large, particularly in the p_x direction. The reason for such large bounds are not only the inevitable computational errors, which in theory can be as small as we like (by taking a smaller time step at the price of a slower computation), but particularly the wrapping effect. See [AZ, GZ] and the references given there for a discussion on this topic. Here we just want to point out that although it is possible by a change of variable to get rid of the singularities, it is not possible to get rid of the wrapping effect in the same way, at least not with the same change of variable.

The first trick we had to adopt consist in computing only half of the Poincaré map at a time, and this is the second reason, in fact the most important, for introducing the maps H_1 and H_2. Indeed the wrapping effect is usually exponential, therefore by considering about half trajectory time it is rather drastically reduced. By this method we obtain a great reduction of the error: of course we have to pay the price of a larger number of computations, but the trade-off is very positive. The second trick that proved to be essential consists in computing the inverse of the map instead of the actual map for some checks, see the definition of back-covering below. This is important whenever some trajectory starts away from the primaries but comes close to one of them at the intersection with the Poincaré plane, indeed in such cases a very short time step is necessary to keep the error small, since close to the singularities the speed undergoes a strong variation while the particle crosses the Poincaré plane. The particle is in fact a point, but in order to compute the Poincaré map we have to consider the envelope of its position with the error bounds, hence it takes a finite time to cross the plane. It turns out that the inverse trajectory, starting close to a primary and ending away from both primaries, raises a much lower error.

5.1. **Topological tools.** The following definitions were introduced in [AZ]. Definitions 5.3 and 5.4 are introduced here for the first time.

Definition 5.1. *A* ***triple set*** *(or t-set) is a triple $N = (|N|, N^l, N^r)$ of closed subsets of $\mathbb{R}^2$ satisfying the following properties:*

1: *$|N|$ is a closed parallelogram*
2: *N^l and N^r are homeomorphic to closed half-planes*
3: *$N^l \cap N^r = \emptyset$*
4: *the sets $N^{le} := N^l \cap |N|$ and $N^{re} := N^r \cap |N|$ are two nonadjacent edges of $|N|$*

We call $|N|$, N^l, N^r, N^{le} and N^{re} the support, the left side, the right side, the left edge and the right edge of the t-set N respectively. One observes that $\mathbb{R}^2 \setminus (|N| \cup N^l \cup N^r)$ consists of two disjoint sets. We call such sets the the top and the bottom of the triple set (N^t and N^b). We also set $N^{te} := N^t \cap |N|$ and $N^{be} := N^b \cap |N|$ (the top and bottom edges of N).

Remark 5.1. Since all theorems we use concern topological properties of the t-sets, then it is clear that any topologically equivalent (homeomorphic) choice of sets will give identical results.

Definition 5.2. *Let $f : \Omega \subset \mathbb{R}^2 \to \mathbb{R}^2$ be a map and let N_1 and N_2 be two triple sets. We say that N_1 $f-$covers N_2 ($N_1 \stackrel{f}{\Longrightarrow} N_2$) if:*

a: $f(|N_1|) \subset \mathrm{int}(N_2^l \cup |N_2| \cup N_2^r)$
b: *either* $f(N_1^{le}) \subset \mathrm{int}(N_2^l)$ *and* $f(N_1^{re}) \subset \mathrm{int}(N_2^r)$
or $f(N_1^{le}) \subset \mathrm{int}(N_2^r)$ *and* $f(N_1^{re}) \subset \mathrm{int}(N_2^l)$

The following lemma says that we can reduce the condition (a) in the above definition to the boundary of $|N_1|$ if we know that the map f is defined on $|N_1|$ and it is injective. This lemma plays a very important role in the computer assisted verification of the covering relations, as it reduces the computations to the boundary of $|N_1|$ (see Section 6 in [GZ], for more details).

Lemma 5.1. *Let $f : \Omega \subset \mathbb{R}^2 \to \mathbb{R}^2$ be a map and let N_1 and N_2 be two triple sets. Assume that f is an injective map on $|N_1|$, then $N_1 \stackrel{f}{\Longrightarrow} N_2$ if and only if*

a′: $f(\partial|N_1|) \subset \mathrm{int}(N_2^l \cup |N_2| \cup N_2^r)$
b: *either* $f(N_1^{le}) \subset \mathrm{int}(N_2^l)$ *and* $f(N_1^{re}) \subset \mathrm{int}(N_2^r)$
or $f(N_1^{le}) \subset \mathrm{int}(N_2^r)$ *and* $f(N_1^{re}) \subset \mathrm{int}(N_2^l)$

As we pointed out above, in some circumstances it is easier to compute the inverse flow, then the direct flow. To exploit this fact we give the following definition:

Definition 5.3. *Let $f : \Omega_1 \subset \mathbb{R}^2 \to \Omega_2 \subset \mathbb{R}^2$ be an invertible map and let N_1 and N_2 be two triple sets. We say that N_1 $f-$backcovers N_2 ($N_1 \stackrel{f}{\Longleftarrow} N_2$) if:*

a: $f^{-1}(|N_2|) \subset \mathrm{int}(N_1^t \cup |N_1| \cup N_1^b)$
b: *either* $f^{-1}(N_2^{te}) \subset \mathrm{int}(N_1^t)$ *and* $f^{-1}(N_2^{be}) \subset \mathrm{int}(N_1^b)$
or $f^{-1}(N_2^{te}) \subset \mathrm{int}(N_1^b)$ *and* $f^{-1}(N_2^{be}) \subset \mathrm{int}(N_1^t)$

We point out that, although covering and backcovering occur often simultaneously and they are indeed a very similar phenomenon, they are not equivalent. In fact it may even happen that a map f is not defined on the whole support of N_1, and still N_1 $f-$backcovers N_2. On the other hand, the result of a backcovering relation is very similar to the result of a covering relation as far as the results we are interested in are concerned, see Lemma 5.3. For this reason we define the generic covering as follows:

Definition 5.4. *Let $f : \Omega_1 \subset \mathbb{R}^2 \to \Omega_2 \subset \mathbb{R}^2$ be an invertible map and let N_1 and N_2 be two triple sets. We say that N_1 generically $f-$covers N_2 ($N_1 \overset{f}{\Longleftrightarrow} N_2$) if N_1 $f-$covers N_2 or N_1 $f-$backcovers N_2.*

Assume that we have n t-sets N_i, $i = 1, \dots, n$, with some covering relations. Let $N = \bigcup_i |N_i|$; the following two definitions are standard.

Definition 5.5. *Let f be injective. The invariant set of N is defined by* $\mathrm{Inv}(N, f) := \{x \in N : f^i(x) \in N$ *for all* $i \in \mathbb{Z}\}$.

Definition 5.6. *The transition matrix $T(j,i)$, $i,j = 1, \dots, n$, is defined as follows:*

$$T(j,i) = \begin{cases} 1 & \text{if } N_i \overset{f}{\Longleftrightarrow} N_j \\ 0 & \text{otherwise} \end{cases}$$

The following theorem follows immediately from Theorem 4 in [Z3] and it is the main topological tool we use:

Theorem 5.2. *Given n t-sets $M_i \subset \mathbb{R}^2$ and n continuous maps $f_i : M_i \to \mathbb{R}^2$, such that*

$$M_0 \overset{f_0}{\Longrightarrow} M_1 \overset{f_1}{\Longrightarrow} M_2 \overset{f_2}{\Longrightarrow} M_2 \dots \overset{f_{n-1}}{\Longrightarrow} M_0 = M_n,$$

then there exists $x \in \mathrm{int}|M_0|$, such that $f_k \circ \dots \circ f_1 \circ f_0(x) \in \mathrm{int}|M_{k+1}|$, for $k = 0, \dots, n-1$ and $x = f_{n-1} \circ \dots \circ f_1 \circ f_0(x)$.

By the following lemma we can extend the previous theorem to the generic backcovering, see Corollary 5.4.

Lemma 5.3. *Let $f : \Omega_1 \subset \mathbb{R}^2 \to \Omega_2 \subset \mathbb{R}^2$ be an invertible map and let N_1 and N_2 be two triple sets. If N_1 $f-$backcovers N_2 then there exists a t-set K such that N_1 $id-$covers K, and K $f-$covers N_2 (id is the identity map in $\mathbb{R}^2$).*

Proof. By definition of backcovering, if N_1 $f-$backcovers N_2, then $f^{-1}(N_2)$ looks as the light grey rectangle in the Figure 3, therefore it is possible to define a t-set K such that the boundary of its support is very close to the boundary of $f^{-1}(N_2)$, in such a way that $N_1 id-$covers K and K $f-$covers N_2. To prove this, just consider a set K' as the dark grey rectangle in the picture, i.e. consider a set slightly smaller than N_2 in the top-down direction and sligthly larger in the left-right direction. By continuity of the map f , if K' is close enough to the support of N_2, then $f^{-1}(K')$ exists. Let the support of K be $f^{-1}(K')$ and define its edges in a suitable way. By this definition K $f-$covers N_2. To complete definition of K and the proof, just define the right and left side of K in such a way that N_1 $id-$covers K. □

Corollary 5.4. *Given t-sets $M_i \subset \mathbb{R}^2$ and continuous maps $f_i : M_i \to \mathbb{R}^2$, such that*

$$M_0 \overset{f_0}{\Longleftrightarrow} M_1 \overset{f_1}{\Longleftrightarrow} M_2 \overset{f_2}{\Longleftrightarrow} M_2 \dots \overset{f_{n-1}}{\Longleftrightarrow} M_0 = M_n,$$

then there exists $x \in \mathrm{int}|M_0|$, such that $f_k \circ \dots \circ f_1 \circ f_0(x) \in \mathrm{int}|M_{k+1}|$, for $k = 0, \dots, n-1$ and $x = f_{n-1} \circ \dots \circ f_1 \circ f_0(x)$.

Let Σ_n be the set of bi-infinite sequences of n symbols

Definition 5.7. *A sequence $\{x_k\} \in \Sigma_n$ is said to be* admissible *if $T(x_{k+1}, x_k) = 1$ for all k. We denote by $\Sigma_A \subset \Sigma_n$ the set of all admissible sequences.*

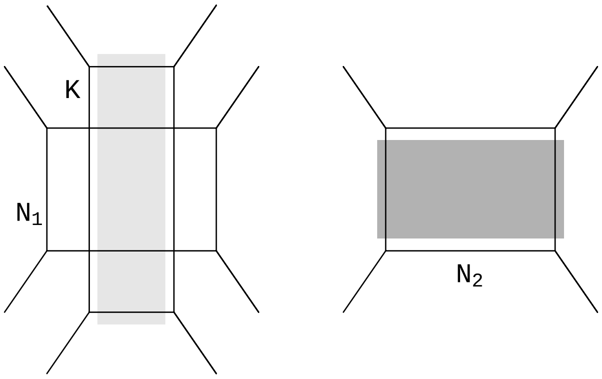

FIGURE 3. In light grey $f^{-1}(N_2)$, in dark grey $K' = f(K)$

Definition 5.8. *Assume $|N_i| \cap |N_j| = \emptyset$, for $i \neq j$. The projection $\pi : \mathrm{Inv}(N, f) \to \Sigma_A$ is defined by setting $\pi(x)_i = j$ where j satisfies $f^i(x) \in |N_j|$ for all $i \in \mathbb{Z}$.*

The set Σ_A inherits the topology from Σ_n; the shift map $\sigma : \Sigma_A \to \Sigma_A$ is continuous. We prove a semiconjugacy between σ and f, i.e. we prove that $\sigma \circ \pi = \pi \circ f|_{\mathrm{Inv}(N,f)}$. In particular this implies that there exists a symbolic dynamics structure on $\mathrm{Inv}(N, f)$.

The following theorem was proved in [Z3] (see Theorems 5 and 6) for the case $n = 2$. The following is a natural extension to a generic number of sets and the proof is exactly the same.

Theorem 5.5. *The projection π is onto, and if $\{x_n\} \in \Sigma_A$ is a periodic sequence, then $\pi^{-1}(\{x_n\})$ contains a periodic point.*

5.2. **Description of the triple sets and euristic results.** In this section of the paper we provide the euristic results we obtained, while in the following section we prove that such results are rigorous. In the remaining part of this paper we fix $h = .3$.

Definition 5.9. *The supports of all triple sets are defined by giving the coordinates of the center (x, y), the length of the sides (l_x, l_y) and the angular coefficients of the sides (α, β) as follows:*

N_0: $(x, y) = (-0.7942, 0.)$, $(l_x, l_y) = (.0065, .0065)$, $(\alpha, \beta) = (.93, -.93)$.
N_1: $(x, y) = (-.7848, .0129)$, $(l_x, l_y) = (.002, .005)$, $(\alpha, \beta) = (-2.136, 2.136)$.
N_2: $(x, y) = (-.7589, .05086)$, $(l_x, l_y) = (.002, .005)$, $(\alpha, \beta) = (-1.811, 1.981)$.
N_3: $(x, y) = (.08, .125)$, $(l_x, l_y) = (.01, .04)$, $(\alpha, \beta) = (1.124, 2.008)$.
N_4: $(x, y) = (.131, .028)$, $(l_x, l_y) = (.007, .007)$, $(\alpha, \beta) = (-2.091, 2.094)$.
N_5: $(x, y) = (.143, .0075)$, $(l_x, l_y) = (.012, .011)$, $(\alpha, \beta) = (-2.09, 2.11)$.
N_6: $(x, y) = (0.1470, 0.)$, $(l_x, l_y) = (.0155, .0155)$, $(\alpha, \beta) = (-2.07, 2.07)$.
K_0: $(x, y) = (0.04873, 0.)$, $(l_x, l_y) = (.0004, .0004)$, $(\alpha, \beta) = (1.818, -1.818)$.
K_1: $(x, y) = (0.04775, 0.)$, $(l_x, l_y) = (.0009, .0009)$, $(\alpha, \beta) = (1.131, -1.131)$.
K_2: $(x, y) = (-0.7365, 0.)$, $(l_x, l_y) = (.0009, .0009)$, $(\alpha, \beta) = (1.817, -1.817)$.
K_3: $(x, y) = (0.04824, 0.)$, $(l_x, l_y) = (.004, .004)$, $(\alpha, \beta) = (1.818, -1.818)$.
K_4: $(x, y) = (0.06712, 0.)$, $(l_x, l_y) = (.01, .01)$, $(\alpha, \beta) = (1.835, -1.835)$.

The left (resp. right) edge of each set is the segments whose end points are $(x + l_x \cos\alpha + l_y \cos\beta, y + l_x \sin\alpha + l_y \sin\beta)$ and $(x + l_x \cos\alpha - l_y \cos\beta, y + l_x \sin\alpha - l_y \sin\beta)$ (resp. $(x - l_x \cos\alpha + l_y \cos\beta, y - l_x \sin\alpha + l_y \sin\beta)$ and $(x - l_x \cos\alpha - l_y \cos\beta, y - l_x \sin\alpha - l_y \sin\beta)$). The boundaries

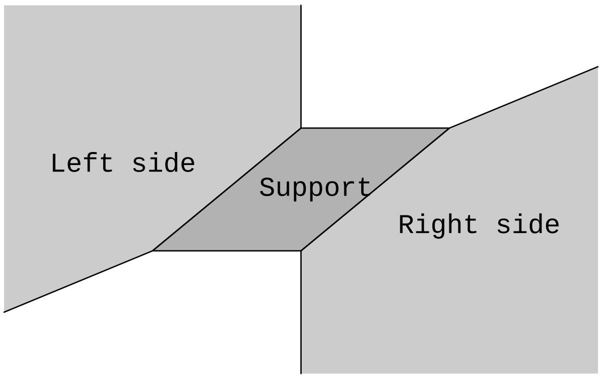

FIGURE 4. An example of a t-set

of the left and right sides of each t-set are the lines crossing two opposite vertices of the support, see Figure 4.

In the following Figures the sets $N_0 - N_6$ and their images through the Poincaré map are represented. The sets are displayed in thick lines, while their images are displayed in thin lines We had to make three different pictures in order to have all sets visible. Note that the scale of the pictures are quite different.

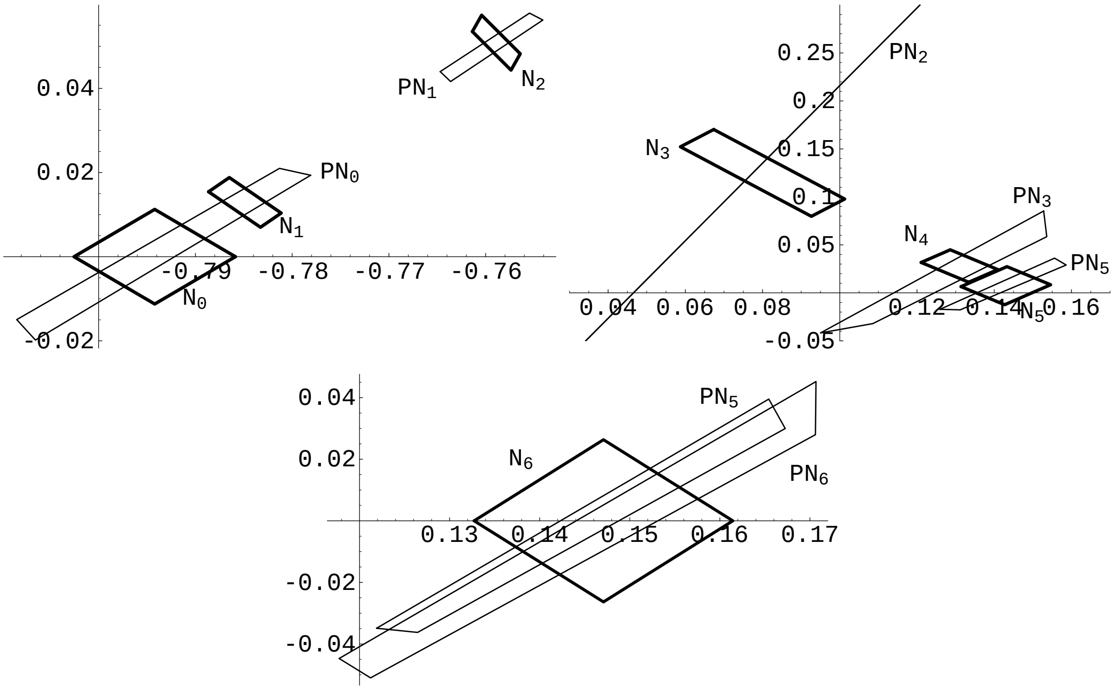

Definition 5.10. *Let M be a t-set. We define its symmetric image with respect to the x-axis $\tilde{M}$ as follows: if $S : \mathbb{R}^2 \to \mathbb{R}^2$ is the map defined by $S(x, y) = (x, -.y)$, let $|\tilde{M}| = S(|M|)$, $\tilde{M}^l = S(M^l)$, $\tilde{M}^r = S(M^r)$, and the remaining definitions follow as in Definition 5.1.*

Lemma 5.6. *Let M_1 and M_2 be t-sets, let $\tilde{M}_1$ and $\tilde{M}_2$ be the sets symmetric with respect to symmetry defined above and assume that $M_1 \overset{P}{\Longrightarrow} M_2$. Then $\tilde{M}_1 \overset{P}{\Longleftarrow} \tilde{M}_2$.*

Proof. This follows by the Definitions 5.2, 5.3, 5.10 and the symmetry of the Poincaré map (see the end of Section 3). □

Remark 5.2. *The supports of the sets N_0, N_6, K_0, K_1, K_2, K_3, K_4 are by definition symmetric with respect to the x axis. We denote $\tilde{N}_i$, $i = 1, \dots 5$, the sets symmetric to the sets N_i with respect to symmetry defined above.*

We denote by $\Longrightarrow$ (resp. $\Longleftarrow$) the covering (resp. the backcovering) with respect to the map P.

The numerical experiments suggest that the following covering relations hold:

$$N_0 \Longrightarrow N_0 \Longrightarrow N_1 \Longrightarrow N_2 \Longrightarrow N_3 \Longrightarrow N_4 \Longrightarrow N_5 \Longrightarrow N_6 \Longrightarrow N_6, \tag{5.1}$$

$$K_0 \Longrightarrow K_0 \Longrightarrow K_3 \Longrightarrow K_3 \Longrightarrow N_3, \tag{5.2}$$

$$K_1 \Longrightarrow K_2 \Longrightarrow K_3, \tag{5.3}$$

$$K_4 \Longrightarrow K_4 \Longrightarrow N_3, \tag{5.4}$$

If these relations could be verified, then by Lemma 5.6 the following covering relations would hold as well:

$$N_6 \Longleftarrow \tilde{N}_5 \Longleftarrow \tilde{N}_4 \Longleftarrow \tilde{N}_3 \Longleftarrow \tilde{N}_2 \Longleftarrow \tilde{N}_1 \Longleftarrow N_0, \tag{5.5}$$

$$\tilde{N}_3 \Longleftarrow K_3 \Longleftarrow K_0, \tag{5.6}$$

$$K_3 \Longleftarrow K_2 \Longleftarrow K_1. \tag{5.7}$$

$$\tilde{N}_3 \Longleftarrow K_4. \tag{5.8}$$

Remark 5.3. The trajectories of some points in the support of the set K_3 appear to collapse into a primary, therefore the support of the set K_3 does not seem to lie in the domain of the Poincaré map, so the statement above is not accurate. What really happens (numerically) is that the support of the set K_3 lies in the domain of H_1, the set K_3 H_1-covers two sets L_3 and M_3 which in turn H_2-cover the sets K_3 and N_3 respectively. For the purposes of Theorem 5.2 and Corollary 5.4 this is equivalent to the coverings described above.

5.3. **Rigorous covering relations.** In order to have covering relations as described in Definition 5.2, we need to be sure that the Poincaré map is defined on the whole support of the t-set. On the other hand, by Lemma 5.1 it is enough to perform rigorous computations on the boundaries of the t-sets, provided that we can prove that the map is defined on the whole supports. This is essential for the rigorous proof to be made in a reasonable time, since to check by computer assistance the definition of the Poincaré map on the supports of the t-sets would be very time consuming. In order to prove that the half Poincaré maps are defined on the supports of all t-sets we argue as follows. We only give the proof for the half Poincaré map H_1, the proof for H_2 being equivalent. First we have to prove that the trajectory does not collide with one primary. Then we observe that the projections of the trajectories we are interested in on the (y, p_y) plane appear to be rotating around either a primary or the Lagrangian point L_1. If we can compute the angular velocity in the (y, p_y) plane and prove that it is bounded away from 0 for long enough time, then it follows that the trajectory has to cross the Poincaré section eventually, hence the map H_1 is well defined. In [AZ] it was possible to prove by analytical computations that the projection on the (x, p_x) plane of all trajectories have positive angular velocity with respect to the origin. For the restricted 3-body problem such a general statement does not hold, therefore we have to proceed with a different method. First we compute the trajectory of the boundary of the t-set with rigorous bounds on the error. The trajectory of the whole boundary describes a "tube" in $\mathbb{R}^4$. More precisely, the intersection of the trajectory of the boundary with any hyperplane $\alpha p_y + \beta y = 0$ bounds a region on the energy surface; the union of all these intersections is the what we call the tube. Since no trajectories can intersect, all trajectories starting in the interior of the support of the t-set have to remain inside the tube. If we can prove that the angular velocity in the interior of the tube is always bounded away from 0, say its absolute value is larger than $\varepsilon > 0$, it follows that the half Poincaré map is well defined on the whole interior of the support of the t-set; indeed any trajectory starting in the interior of the t-set must intersect the Poincaré plane in a time $T \leq \pi/\varepsilon$.

For a given point $(x, p_x) \in \partial N$ let

$$\Phi(x, p_x) = \varphi(x, p_x; [0, T_1]),$$

where φ is the map defined in Section 3 and $T_1 = T_1(x, p_x)$ is the half Poincaré time also defined in Section 3. $\Phi(x, p_x)$ is the trajectory of the point $(x, p_x, 0, \sqrt{2\Omega(x,0) + h - p_x^2})$ under the flow induced by the equations from time 0 to the time T_1 when it reaches the Poincaré plane. If we can prove that $H_1(\partial N)$ exists, since the flows of two different points cannot intersect, unless they coincide, then $H_1(\partial N)$ bounds a region M in the Poincaré plane. We want to prove that H_1 is defined on the whole set $|N|$ and $H_1(|N|) = M$. Let $\Sigma = |N| \cup \bigcup_{(x,p_x)\in\partial N} \Phi(x, p_x) \cup M$. The hypersurface $\Sigma \subset \mathbb{R}^4$ divides $\mathbb{R}^4$ into two connected regions; call Ξ the bounded region. It is clear that for all $(x, p_x) \in |N| \setminus \partial N$ either there exists $H_1(x, p_x)$, or $\varphi\left(x, p_x, 0, \sqrt{2\Omega(x,0) + h - p_x^2}; T\right) \in \Xi$ for all $T \geq 0$. Let $\beta(x, p_x, y, p_y) = (2p_x + \Omega_y(x, y))y - p_y^2$. The next Lemma shows that, if Ξ does not intersects the plane $(y = 0,\ p_y = 0)$ and $|\beta(x, p_x, y, p_y)| \geq \delta > 0$ for all $(x, p_x, y, p_y) \in \Xi$, then the second case cannot happen.

Lemma 5.7. *Fix h and (x, p_x) such that $x \neq \{R_1, -R_2\}$ and $2\Omega(x,0) + h - p_x^2 > 0$; let $p_y = \sqrt{2\Omega(x,0) + h - p_x^2}$. Let $(x(T), p_x(t), y(T), p_y(T)) = \varphi(x, p_x, 0, p_y; T)$ be the flow induced by (1.1); let $\beta(T) = (2p_x(T) + \Omega_y(x(T), y(T)))y(T) - p_y^2(T)$. If $y^2(T) + p_y^2(T) > 0$ and $|\beta(T)| \geq \delta$ for all T and some $\delta > 0$, then the half Poincaré maps H_1 and H_2 in (x, p_x) are well defined.*

Proof. Since $y^2(T)+p_y^2(T)>0$ we can use polar coordinates. Let $\alpha(T)$ be the angle. Taking the derivative we have

$$\dot\alpha=\frac{\dot p_y y-p_y^2}{y^2+p_y^2}=\frac{(2p_x+\Omega_x)y-p_y^2}{y^2+p_y^2}.$$

Since $y^2+p_y^2$ is bounded and $(2p_x+\Omega_x)y-p_y^2$ is bounded away from 0, then for some T we have $|\alpha(T)-\alpha(0)|>\pi$, therefore the map is defined. □

Lemma 5.8. *There exists $\delta>0$ such that $\beta(x,p_x,y,p_y)\le-\delta$ for all $(x,p_x,y,p_y)\in\Xi$, there Ξ is the tube corresponding to any of the t-sets defined in Definition 5.9.*

Proof. The proof is by computer assistance and it is performed with the following procedure. Choose a t-set and let (x,p_x) the middle point of its support. Let $\bar\varphi(x,p_x,t)$ be the approximate flow, computed by some suitable algorithm (we used Mathematica 4.0 for this purpose). Let $\bar T_1$ be the approximate Poincaré time, i.e. $\bar\varphi_3(x,p_x,t)>0$ for all $0<t<\bar T_1$ and $\bar\varphi_3(x,p_x,\bar T_1)=0$. For an integer $N>0$ let $t_i=i\bar T_1/N$, $i=0,N$,

$$\bar\Xi_i=\left\{(x,p_x,y,p_y)\in\mathbb{R}^4:d((x,p_x,y,p_y),\bar\varphi(x,p_x,t_i))\le1\right\},$$

where d is a distance in $\mathbb{R}^4$ defined by

$$d((x^1,p_x^1,y^1,p_y^1),(x^2,p_x^2,y^2,p_y^2))=\max(a_1|x^1-x^2|,a_2|p_x^1-p_x^2|,a_3|y^1-y^2|,a_4|p_y^1-p_y^2|)$$

and $\{a_i\}$ are positive constants. Let

$$\bar\Xi=\bigcup_{i=0,N}\bar\Xi_i.$$

$\bar\Xi$ is a very rough approximation of the flow of the support of the t-set. If all the constants entering in the definition of $\bar\Xi$ are chosen appropriately, one can expect that the true trajectory of the support of the t-set is entirely contained in $\bar\Xi$. With computer assistance we checked rigorously that the true trajectory of the boundary of the t-sets never leaves $\bar\Xi$. Using interval arithmetics algorithms we can compute

$$\delta_i=\max_{(x,p_x,y,p_y)\in\bar\Xi_i}\beta(x,p_x,y,p_y).$$

If $\max_i\delta_i<0$ the proof is complete. □

As we pointed out before, it is not convenient to check directly the covering relations given in the previous section, since that would require an enormous amount of computer time. Furthermore, by Remark 5.3 one of those relations does not hold as it is stated. This problem is due to the fact that, even if we start from a very small interval in the computation of the Poincaré map, the error and the wrapping effect accumulated in the Poincaré time is quite large. Instead we prefer to define some auxiliary t-sets on the symmetric Poincaré plane, i.e. the plane $y=0$, $\dot y<0$, and prove the covering relations given below:

$$M_0\overset{H_2}{\Longrightarrow}N_0\overset{H_1}{\Longrightarrow}M_0\overset{H_2}{\Longrightarrow}N_1\overset{H_1}{\Longrightarrow}M_1\overset{H_2}{\Longrightarrow}N_2\overset{H_1}{\Longrightarrow}M_2\overset{H_2}{\Longrightarrow}N_3$$

$$\overset{H_1}{\Longrightarrow}M_4\overset{H_2}{\Longrightarrow}N_4\overset{H_1}{\Longrightarrow}M_5\overset{H_2}{\Longrightarrow}N_5\overset{H_1}{\Longrightarrow}M_6\overset{H_2}{\Longrightarrow}N_6\overset{H_1}{\Longrightarrow}M_6$$

$$L_0\overset{H_2}{\Longrightarrow}K_0\overset{H_1}{\Longrightarrow}L_0\overset{H_2}{\Longrightarrow}K_3\overset{H_1}{\Longrightarrow}L_3\overset{H_2}{\Longrightarrow}K_3\overset{H_1}{\Longrightarrow}M_3$$

$$K_1\overset{H_1}{\Longrightarrow}L_1\overset{H_2}{\Longrightarrow}K_2\overset{H_1}{\Longrightarrow}L_2\overset{H_2}{\Longrightarrow}K_3$$

$$K_4\overset{H_1}{\Longrightarrow}L_4\overset{H_2}{\Longrightarrow}K_4\overset{H_1}{\Longrightarrow}L_5\overset{H_2}{\Longrightarrow}N_3$$

But even to prove these covering relations with the half Poincaré maps turns out to be a difficult task, indeed some of the sets are quite close to the primaries, and this causes the computation of rigorous bounds for the intersection of the trajectory with the Poincaré plane to be critical. To overcome this difficulty we have to use the alternative, but equivalent, definition of covering through the inverse of the Poincaré map, see Definition 5.3. The following Lemma states the covering relations we actually prove by computer assistance:

Lemma 5.9.

$$M_0 \overset{H_2}{\Longleftarrow} N_0 \overset{H_1}{\Longrightarrow} M_0 \overset{H_2}{\Longleftarrow} N_1 \overset{H_1}{\Longrightarrow} M_1 \overset{H_2}{\Longleftarrow} N_2 \overset{H_1}{\Longrightarrow} M_2 \overset{H_2}{\Longrightarrow} N_3$$
$$\overset{H_1}{\Longleftarrow} M_4 \overset{H_2}{\Longrightarrow} N_4 \overset{H_1}{\Longleftarrow} M_5 \overset{H_2}{\Longrightarrow} N_5 \overset{H_1}{\Longleftarrow} M_6 \overset{H_2}{\Longrightarrow} N_6 \overset{H_1}{\Longleftarrow} M_6$$

$$L_0 \overset{H_2}{\Longleftarrow} K_0 \overset{H_1}{\Longrightarrow} L_0 \overset{H_2}{\Longrightarrow} K_3 \overset{H_1}{\Longrightarrow} L_3 \overset{H_2}{\Longrightarrow} K_3 \overset{H_1}{\Longrightarrow} M_3$$
$$K_1 \overset{H_1}{\Longrightarrow} L_1 \overset{H_2}{\Longleftarrow} K_2 \overset{H_1}{\Longrightarrow} L_2 \overset{H_2}{\Longrightarrow} K_3$$
$$K_4 \overset{H_1}{\Longleftarrow} L_4 \overset{H_2}{\Longrightarrow} K_4 \overset{H_1}{\Longleftarrow} L_5 \overset{H_2}{\Longrightarrow} N_3$$

5.4. **Topological entropy estimates.** We want to estimate the topological entropy of the map P. To this purpose we use the following lemma:

Lemma 5.10. *Let $f : X \to X$ be a continuous map. Let $S \subset X$ be an invariant set, let A be an $n \times n$ matrix such that there exists a surjective map $\pi : S \to \Sigma_A$ satisfying $\sigma \circ \pi = \pi \circ f$. Then the topological entropy of f is larger than $\ln(\max\{|\lambda_i|, \quad \lambda_i$ is an eigenvalue of $A\}$.*

Proof. The proof is an easy consequence of Theorem 7.13 in [WA] and is left to the reader. □

Corollary 5.11. *The topological entropy of P is larger then* 2.59131.

Proof. Consider the collection of t-sets N_0, N_1, N_2, N_3, N_4, N_5, N_6, $\tilde{N}_1$, $\tilde{N}_2$, $\tilde{N}_3$, $\tilde{N}_4$, $\tilde{N}_5$, K_0, K_1, K_2, K_3, K_4. Let A be the transition matrix resulting from Lemma 5.9: we have

$$A = \begin{bmatrix}
1 & 1 & 0 & 0 & 0 & 0 & 0 & 0 & 0 & 0 & 0 & 0 & 0 & 0 & 0 & 0 & 0 \\
0 & 0 & 1 & 0 & 0 & 0 & 0 & 0 & 0 & 0 & 0 & 0 & 0 & 0 & 0 & 0 & 0 \\
0 & 0 & 0 & 1 & 0 & 0 & 0 & 0 & 0 & 0 & 0 & 0 & 0 & 0 & 0 & 0 & 0 \\
0 & 0 & 0 & 0 & 1 & 0 & 0 & 0 & 0 & 0 & 0 & 0 & 0 & 0 & 0 & 0 & 0 \\
0 & 0 & 0 & 0 & 0 & 1 & 0 & 0 & 0 & 0 & 0 & 0 & 0 & 0 & 0 & 0 & 0 \\
0 & 0 & 0 & 0 & 0 & 0 & 1 & 0 & 0 & 0 & 0 & 0 & 0 & 0 & 0 & 0 & 0 \\
0 & 0 & 0 & 0 & 0 & 0 & 1 & 0 & 0 & 0 & 0 & 1 & 0 & 0 & 0 & 0 & 0 \\
1 & 0 & 0 & 0 & 0 & 0 & 0 & 0 & 0 & 0 & 0 & 0 & 0 & 0 & 0 & 0 & 0 \\
0 & 0 & 0 & 0 & 0 & 0 & 0 & 1 & 0 & 0 & 0 & 0 & 0 & 0 & 0 & 0 & 0 \\
0 & 0 & 0 & 0 & 0 & 0 & 0 & 0 & 1 & 0 & 0 & 0 & 0 & 0 & 0 & 0 & 0 \\
0 & 0 & 0 & 0 & 0 & 0 & 0 & 0 & 0 & 1 & 0 & 0 & 0 & 0 & 0 & 0 & 0 \\
0 & 0 & 0 & 0 & 0 & 0 & 0 & 0 & 0 & 0 & 1 & 0 & 0 & 0 & 1 & 0 & 1 \\
0 & 0 & 0 & 0 & 0 & 0 & 0 & 0 & 0 & 0 & 0 & 0 & 1 & 0 & 0 & 1 & 0 \\
0 & 0 & 0 & 0 & 0 & 0 & 0 & 0 & 0 & 0 & 0 & 0 & 0 & 0 & 1 & 0 & 0 \\
0 & 0 & 0 & 0 & 0 & 0 & 0 & 0 & 0 & 0 & 0 & 0 & 0 & 1 & 0 & 1 & 0 \\
0 & 0 & 0 & 0 & 0 & 0 & 0 & 0 & 0 & 1 & 0 & 0 & 1 & 0 & 1 & 1 & 0 \\
0 & 0 & 0 & 0 & 0 & 0 & 0 & 0 & 0 & 1 & 0 & 0 & 0 & 0 & 0 & 0 & 1
\end{bmatrix}.$$

By Lemma 5.10 a lower bound for h_t is given by the maximal norm eigenvalue of the matrix A. The characteristic polynomial is

$$p(x) = -3\,x + 5\,x^2 - 3\,x^4 + x^5 - x^9 + 7\,x^{10} - 10\,x^{11} \\ - 6\,x^{12} + 21\,x^{13} - 10\,x^{14} - 5\,x^{15} + 5\,x^{16} - x^{17},$$

and since $p(2.59131) = 1.94022$ and $p(2.59132) = -5.61369$, then $h_t(P) > 2.59131$. □

5.5. **Symbolic dynamics.** By Lemma 5.9 the sets N_0, N_6, K_0, K_1 and K_4 $P-$cover themselves (more precisely K_1 P^2-covers itself), hence there exists (at least) a periodic orbit for each of these sets which crosses the hyperplane $y = 0$ in the set (or alternatively in the sets K_1 and K_2). The orbit crossing N_0 corresponds to the orbit symmetric to U_2 with respect to the y axis, while orbits N_5, K_0, K_1 and K_4 correspond to the classes U_2, L, D_1 and U_1 respectively. We say that those orbits "correspond to" and not "are", since without considering the derivative of the Poincaré map we cannot exclude that other periodic orbits cross those t-sets. By Theorem 5.5 for all admissible biinfinite sequences of five symbols there exists a solution of equation (1.1) which crosses the t-sets in the same order.

6. Further developments

Although the 3-body problem is very old, there are still many open problems. Computer assisted techniques can help to give rigorous proofs to conjectures. In this paper we gave results that required only C^0 computations. In a forthcoming paper we will discuss further the dependence of the results presented in this paper to the ratio of the masses of the primaries, we will give a rigorous proof of the linear stability or instability of the periodic orbits and we will prove that bifurcations occur with the energy as a parameter value.

7. Computational details

In order to compute the half-Poincaré maps with rigorous bounds we used a fourth order Taylor method. The wrapping effect has been contained by the Lohner algorithm [L]. The typical time step used in the computation of the images of the t-sets is $dt = 10^{-3}$, but in few cases we had to use some lower value, down to $dt = 10^{-4}$. Each side of the t-sets has been divided in 500 to 2000 segments, depending on the apparent value of the Lipschitz constant of the map in the area considered. In a few difficult cases we had to divide each side of a t-set in 5000 segments. Most of the computations used to obtain the bounds for the location of the orbits in Table 1 used $dt = 5.10^{-6}$, but occasionally the time step has been down to 10^{-6}. The whole algorithm has been implemented by a combination of Mathematica and C++ under the Linux O.S. More precisely, Mathematica has been used to handle all the data and to perform most of the parts of the algorithm which are less demanding for the CPU, but more complicated to implement. Furthermore Mathematica has been used to make all numerical experiment, to store the data concerning the t-sets and to draw the pictures. On the other hand C++ has been used for the heavy interval arithmetic computations, where it offered a much better speed. The connection between the two languages is obtained by MathLink. We wish to point out that the full proof took two months of CPU time on a machine equipped with a 1GHz Athlon processor: a full C++ algorithm would probably reduce the time, at the price of a much more complicated and less user frieldly programming. On the other hand, the original algorithm written completely in Mathematica is at least 3-4 times slower. We think that this sharing of task is almost optimal, as far as computational speed and simplicity of programming and data handling is concerned.

Acknowledgement. The author is very grateful to P. Zgliczyński for many discussions and for the interval arithmetic C++ libraries.

References

[AGT] G. Arioli, F. Gazzola, S. Terracini, *Minimization properties of Hill's orbits and applications to some N-body problems*, Ann. Inst. Henri Poincaré, Analyse non linéaire 17, 5 (2000) 617-650

[AZ] G. Arioli, P. Zgliczyński, *Symbolic dynamics for the Hénon-Heiles Hamiltonian on the critical level*, J. Diff. Eq. 171 (2001) 173-202

[GH] J. Guckenheimer, P. Holmes *Nonlinear Oscillations, Dynamical Systems, and Bifurcations of Vector Fields* Springer-Verlag, New York-Heidelberg-Berlin

[GZ] Z. Galias , P. Zgliczyński, Computer assisted proof of chaos in the Lorenz system, Physica D, 115, 1998,165–188

[L] R.J. Lohner, *Computation of Guaranteed Enclosures for the Solutions of Ordinary Initial and Boundary Value Problems*, in: Computational Ordinary Differential Equations, J.R. Cash, I. Gladwell Eds., Clarendon Press, Oxford, 1992.

[MH] Meyer K.R., Hall G.R., Introduction to Hamiltonian Dynamical Systems and the N-body problem, Springer Verlag, 1991

[MM1] K. Mischaikow , M. Mrozek, *Isolating neighborhoods and chaos*, Japan J. Indust. Appl. Math., 12 (1995), 205–236

[MM2] K. Mischaikow , M. Mrozek, *Chaos in the Lorenz equations: A computer assisted proof*, BAMS, 32 (1995), 66–72

[MM3] K. Mischaikow , M. Mrozek, *Chaos in the Lorenz equations: A computer assisted proof. Part II: Details*, Mathematics of Computation, 67, (1998), 1023–1046

[M] Moser J., Stable and random motions in Dynamical Systems, Princeton Univ. Press, 1973

[MS] Moser J., Siegel C.M., Lectures on celestial mechanics, Springer Verlag, 1971

[S] V. Szebehely, Theory of orbits, Academic Press, 1967

[WA] P. Walters, *An Introduction to Ergodic Theory*, Springer Verlag New York, 1982

[W] M. Willem, Minimax Theorems, Birkhäuser, Boston, 1996.

[Z1] P. Zgliczyński, *Fixed point index for iterations, topological horseshoe and chaos,* Topological Methods in Nonlinear Analysis, 1996, Vol. 8, No. 1, 169–177

[Z2] P. Zgliczyński, *Computer assisted proof of chaos in the Hénon map and in the Rössler equations,* Nonlinearity, 1997, Vol. 10, No. 1, 243–252

[Z3] P. Zgliczyński, *Sharkovskii's Theorem for multidimensional perturbations of 1-dim maps*, Ergod. Th. & Dynam. Sys. (1999), 19, 1655-1684

Dipartimento di Scienze e T.A., C.so Borsalino 54, 15100 Alessandria Italy
E-mail address: gianni@unipmn.it *Web page:* http://www.mfn.unipmn.it/~gianni